ETH Zürich

Quantum Device Lab

Semester Thesis

Collimation of metastable 2^3S_1 helium atoms using laser cooling techniques

---

Author:
Max Melchner von Dydiowa

Supervisor:
Tobias Thiele

Principal Investigator:
Prof. Dr. Andreas Wallraff

June 2014

Abstract

By using laser cooling methods we were able to collimate a beam of triplet-state helium 2^3S_1 atoms, thereby reducing its divergence angle from 2.15° to 0.1°. We achieved a 400-fold increase in the beam flux of triplet helium from initially $I_0 = (1.184 \pm 0.032) \times 10^9\,\mathrm{sr}^{-1}\,\mathrm{s}^{-1}$ to approximately $I_{collimated} \approx 5 \times 10^{11}\,\mathrm{sr}^{-1}\,\mathrm{s}^{-1}$.

Contents

1 Introduction

1.1 Rydberg Experiment

The Rydberg experiment studies helium atoms excited to Rydberg states (with principal quantum numbers $n \approx$ 30-40) with typical transition frequencies in the microwave regime. This in principle allows to couple them strongly to photons in chip-based microwave resonators [1, 2]. Rydberg atoms are created in two steps. First, helium is led into a gaseous discharge, where it is excited to the 2^1S_0 (singlet-)state and 2^3S_1 (triplet-)state. The singlet-state helium atoms are subsequently excited to Rydberg states with a UV-laser (312 nm) and then interact with patterned surfaces. Rydberg atoms can be regarded as two-level quantum systems with their ground state and excited state being n^1S_0 and n^1P_0 (n being the principal quantum number) respectively. Microwave transitions between the ground state and excited state are especially interesting because they have a low rate of spontaneous decay, allowing observation of coherent evolution of the two-level quantum system (i.e. Rabi-oscillations) driven by the microwave photons or vacuum in a resonator [3]. After the Rydberg atoms interact with the microwave resonator, they are ionized and detected. The ultimate goal is to have these qubits (coherent Rydberg atoms) interact with the microwave chip. The purpose of the new helium source, which is the subject of this thesis, is to create a high intensity beam of "clean" (i.e. uncontaminated by other states) triplet-state helium atoms to ultimately replace the current singlet-state helium source.

1.2 Advantages of Triplet-State Helium

The use of triplet-state helium has many advantages over singlet-state helium. One reason for using triplet-state helium is its long lifetime of around 7900 s [4] compared to singlet-helium, whose lifetime is about 20 ms [5]. The Rydberg-states of triplet-state helium are thus also longer lived than those of singlet-state helium. This results in longer coherence times of the Rydberg atoms. Secondly, the triplet-state has a closed optical transition between the 2^3S_1 and the $2^3P_{0,1,2}$ states. This makes it possible to collimate the triplet atoms and deflect them using laser forces (see Section 2 for more information), allowing increased density through collimation and filtration of the triplet atoms through deflection [6]. The singlet helium does not have a closed optical transition, making it impossible to separate singlet atoms from unwanted particles such as other states, electrons, protons and photons generated in the source with the metastable atoms. To obtain metastable singlet and triplet helium

atoms, we currently use an electric discharge. Another advantage of triplet-state helium over singlet-state helium is that ≈90% [7, 8] of the metastable atoms created in the discharge are in the triplet state, which means that the yield is much higher than for singlet-state helium. Finally, the Rydberg s and p states of triplet-state helium are less sensitive to electric fields because of a large quantum defect [9], which is vitally important due to high electric fields close to the surface of the chip containing the (superconducting) microwave resonator.

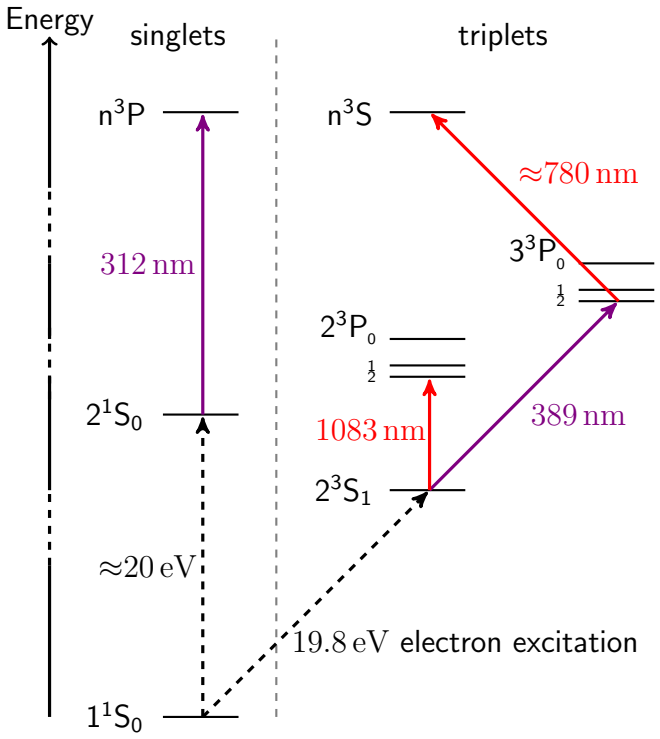

Figure 1 – Optical level scheme of Helium.

1.3 Goals of this Thesis/Accomplishments

The goal of my three weeks at the Quantum Device Lab was to achieve collimation of the triplet-state helium atoms in the new helium source using laser cooling methods. This included finding the best operation parameters (such as laser power, discharge current, etc.) to achieve optimal collimation.

2 Theory

2.1 Photon Kick

The principle behind the collimation setup is to reduce the transverse velocity of atoms coming from the skimmer by using laser cooling techniques. The laser creates a so-called "optical molasses" which, as the name implies, creates a force on atoms moving inside this "molasses". To understand the effect that the laser has on the helium atoms, let us first consider an arbitrary atom which has two distinct energy levels: the ground state (with energy E_g) and the excited state (with energy E_e). When the atom is in its ground state it is excited to the excited state by absorbing a photon with an energy equal to $E_e - E_g$. When the atom is in the excited state it can either be deexcited by stimulated emission (i.e. by another impinging photon) or it will decay after a characteristic lifetime. Both processes result in the emission of a photon with energy $E_e - E_g$. Because photons have momentum, atoms experience a "kick" every time they absorb or emit a photon. Now we can imagine that there is a beam of photons impinging on the atom from a distinct direction, so that when the atom has decayed, it is immediately excited again. Every time a photon is absorbed by the atom, the atom is accelerated in the direction in which the photons are moving ("kick"). If the atom decays via stimulated emission, the atom is accelerated back to its original state before it was excited. However, if the atom decays via spontaneous emission, the photon is emitted randomly in any direction. Because the direction in which spontaneously emitted photons travel is random, the average "kick" the atom receives from spontaneously emitted photons is zero. So while the atom receives a directed "kick" each time it is excited, on average it only receives a half "kick" when decaying back into the ground state. Therefore a laser beam can effectively exert a directed force on an atom, which is equal to: $\frac{1}{2}\hbar k\Gamma$, where $\frac{1}{2}$ is from the population of the excited state, $\hbar k$ is the momentum of the photon and Γ is the inverse lifetime of the excited state.

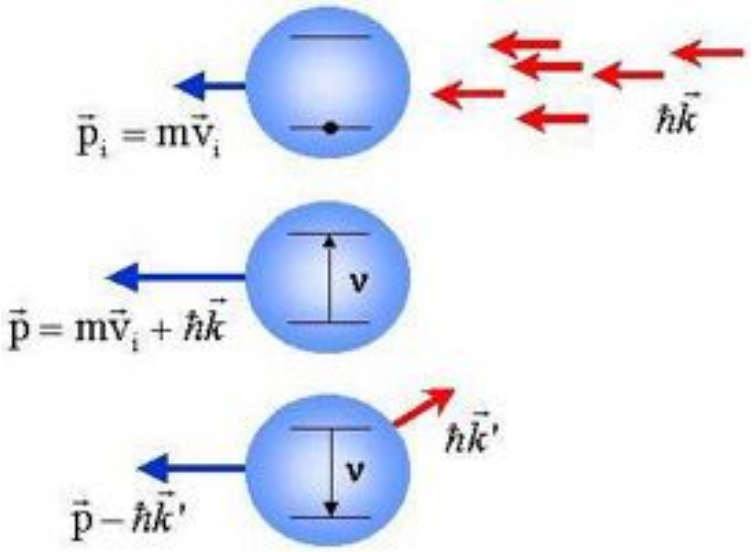

Figure 2 – Visualization of photon-atom interaction. First the atom absorbs a photon and receives a directed acceleration in the photon direction. Later it spontaneously decays and receives a kick in a random direction. [10]

2.2 Doppler shift/Detuning

The Doppler shift describes the effect of movement on the transmission and reception of electromagnetic or acoustic waves. When a transmitter and a receiver of electromagnetic waves are moving, the wavelength that the transmitter transmits and the receiver receives are generally different from when they are at rest. When transmitter and receiver are moving toward/away from each other the receiver is going to perceive a wave with higher/lower frequency (and therefore smaller/larger wavelength) than at rest. This same phenomenon is present when atoms are moving toward a laser source. The atom moving toward the laser source observes that the laser in its inertial system has a shorter wavelength than in the inertial system of the laboratory. This means that even though a laser might have the right frequency to excite the atom from its ground state to its excited state (i.e. it is resonant with the optical transition), a moving atom generally will not be excited, since it observes the photon as having a different frequency than needed for excitation. The Doppler frequency detuning is given in first order (for $|\vec{v}| \ll c$) by $\delta = -\vec{k}\vec{v}$, where $\vec{v}$ is the atom's velocity and $\vec{k}$ is the laser's wave number (see Appendix A for a detailed calculation).

2.3 Laser Force

The force that a single atom experiences from absorbing photons is equal to the time-derivative of the gain in momentum. This, on the other hand, is equal to the number of photon-kicks per second. The force that a laser beam exerts on an atom is given by:

$$F = n_e \hbar k \Gamma$$

We can imagine that the density of the photons (which is proportional to the intensity) is so large that any atom in the ground state is immediately excited. The number of excitations of a single atom per second is therefore only dependent on the lifetime of the excited state $\tau = \frac{1}{\Gamma}$, Γ being the linewidth of the transition. A single photon carries a momentum of $p = \hbar k$ (with $\hbar$-reduced Planck Constant, k-photon wavenumber). In a two-level system, the population of the excited state (relative to the sum of excited and ground state atoms) can only reach a maximum value of $n_e = 0.5$. The population of the excited state can be determined as a function of laser power and detuning, by solving the optical Bloch Equations [3]. For a detailed deduction of n_e, see [11, 12]. The limit is reached when the excitation rate is equal to the rate of stimulated emission and is achieved as the laser power tends towards infinity. Since the laser power in our experiment is much greater than the saturation intensity, the laser force is approximately given by $F = \frac{1}{2}\hbar k \Gamma$.

The cooling of atoms through the stimulation of an optical transition has a fundamental limit, called the Doppler-limit, below which the atoms cannot be cooled using the optical molasses technique (they could however be cooled below this limit with, e.g., polarization gradients or Sisyphus cooling). This limit arises from the random walk in momentum space that the atom undergoes due to spontaneous emission, when the momentum of the atom is on the order of one photon momentum. At the Doppler limit, the directed laser force can only cancel out the momentum gain resulting from random spontaneous emission. The mean velocity of atoms cooled to the Doppler limit in one dimension is given by $v = \frac{\hbar\Gamma}{2m}$ (where m is the mass of a single atom), which is equivalent to a temperature of $T = \frac{\hbar\Gamma}{2k_B}$ [3].

3 Helium Source Setup

3.1 Laser Setup

A fiber laser creates a CW, narrow linewidth (≈70 kHz) infrared laser beam at a wavelength of 1083.33 nm and a power of ≈10 mW, which is split into two separate beams. The first beam is used for Doppler-free saturated helium spectroscopy [3, 11, 12], which is needed to lock the laser wavelength to the 2^3S_1 - 2^3P_2 transition of helium. The error signal is generated with the Pound-Drever-Hall-method [11, 13]. This transition has the lowest energy of the three transitions from $^3S_1$ to $^3P_{0,1,2}$ and corresponds to a wavelength of ≈1083.335 nm [14]. The other beam is amplified to a power between 1100 mW and 3000 mW, and is directed to a setup of mirrors and beam splitters, where the laser is coupled into 3 fibers, two of which are used for collimation and one which is used for deflection (see Figure 3). Currently, we are using two multi-mode fibers for collimation and one single-mode fiber for deflection. To adjust the laser power used for collimation and for deflection, a lambda-half plate and a polarizing beam-splitter were used to split the laser beam. We covered the entire laser setup with a box of thick black cardboard to prevent stray laser radiation from escaping the optical setup. We probed the efficiency of coupling into the three fibers by connecting one end of a fiber to the respective input coupler and the other to a power meter. After optimal adjustment we typically reached an efficiency of 50%, i.e. 50% of the incident laser radiation was coupled into the fiber. Every morning the mirrors and input couplers had to be readjusted because the coupling efficiency usually fell drastically during the night. We believe that this is due to temperature fluctuations or stress in the fiber output coupler. This will be remedied however, by using more stable input/output couplers.

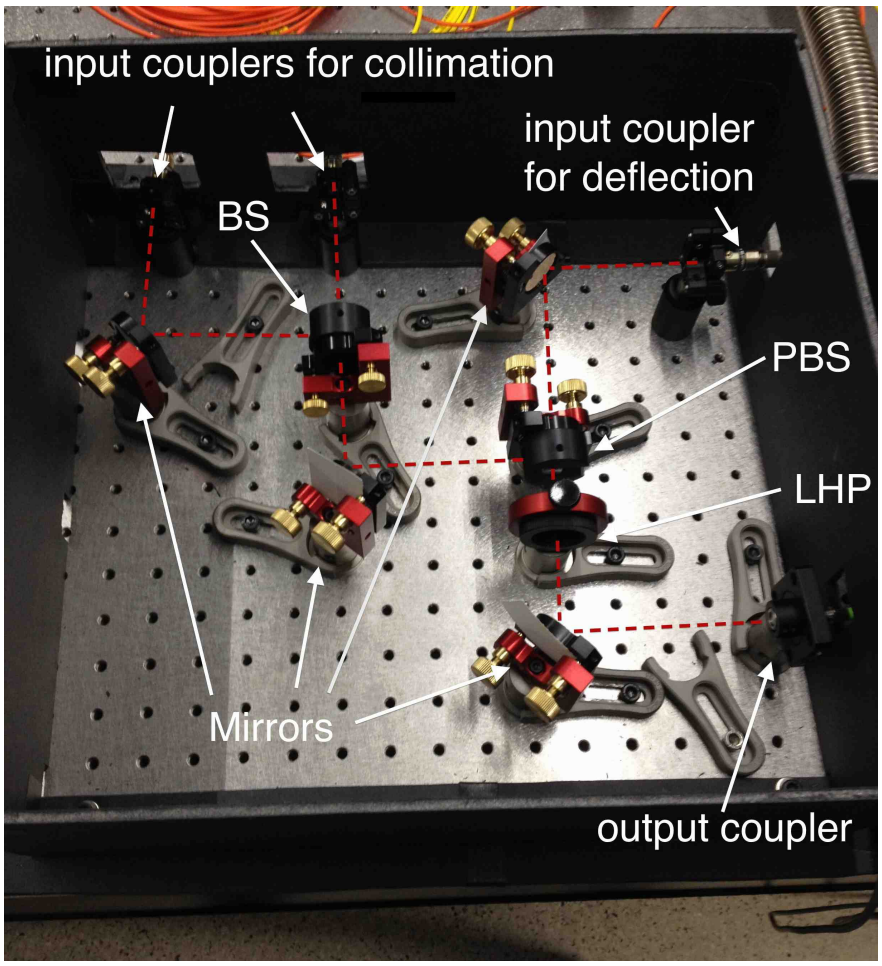

Figure 3 – picture of current laser setup. The dotted red line shows the beam path, which begins at the output coupler. Abbreviations: BS: beam splitter, LHP: lambda-half plate, PBS: polarizing beam splitter

3.2 Source Setup

Ground-state helium is pulsed at a rate of 25 Hz and expands adiabatically through a nozzle (0.5 mm ø) from a high-pressure reservoir (6 bar) into vacuum ($\approx 10^{-7}$ mbar). An electric discharge is mounted right behind this opening. The electric discharge is composed of a tungsten wire carrying a current from 5-6.5A and a pointed metal electrode to which a voltage of 200 V-350 V is applied. Electrons are released from the wire and travel through the helium beam in the direction of the nozzle. When an electron interacts with a helium atom, it can excite or ionize the helium atom by impact. This discharge creates singlet and triplet state helium atoms with a yield of about 10^{-6}. After passing the electric discharge, the atomic beam passes through a first skimmer [12] with a diameter of 2 mm, placed 6 cm from

the tube opening, and through a second skimmer with a diameter of 1 mm, positioned 14 cm from the tube opening. After another 34 mm they enter the collimation chamber (Figure 4). Helium atoms that escape the nozzle have a mean longitudinal velocity of around ≈1700 meters per second and a maximum transverse velocity of about 32 meters per second after they pass the skimmers, which translates to a beam divergence of $\alpha \approx 2.15°$.

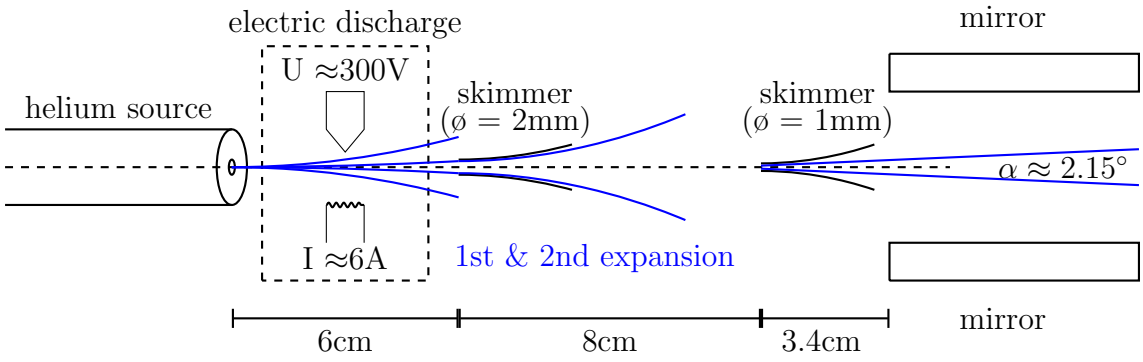

Figure 4 – discharge/skimmer setup

3.3 Collimation/Deflection Setup

The collimation chamber is an evacuated metal rectangular box with a length of 34 cm and with glass windows (length: 28 cm) stretching horizontally along each of its faces. Attached outside of each window is a highly reflective mirror with a length of 15 cm (see Figure 5 (a)). The amplified laser from the laser setup is led through a fiber to an output coupler, where the laser is released onto a mirror. The laser reflects off the mirror into the collimation chamber. After the beam traverses the collimation chamber, it reflects off the mirror attached outside the chamber window (on the opposite side of the output coupler) and propagates back through the collimation chamber to the side which the output coupler is on and reflects off the mirror (see Figure 5 (b)). The beam is thus reflected many times along the length of the collimation chamber and intersects the helium beam with varying angles, creating the optical molasses that we need for collimation [14]. The same setup is also used for vertical collimation. By having the laser impinging from both sides onto the beam of metastable helium (which creates a directed force), the helium beam is collimated. The mirrors are slightly tilted, so that the edges of the mirrors that are farther from the helium source are closer together. This mirror alignment progressively changes the incident angle of the laser onto the helium atoms, which makes the laser resonant with increasingly smaller transverse velocity classes. Therefore the transverse velocity of the helium beam is progressively reduced along

the entire length of the collimation cube (Figure 5). Further along the beam propagation axis, behind the mirrors used for collimation, the deflection setup is attached on one side of the collimation chamber. Deflection is achieved in the same manner as collimation, with the laser creating a directed force on the triplet state helium atoms, thereby separating them from the other metastable atoms [6].

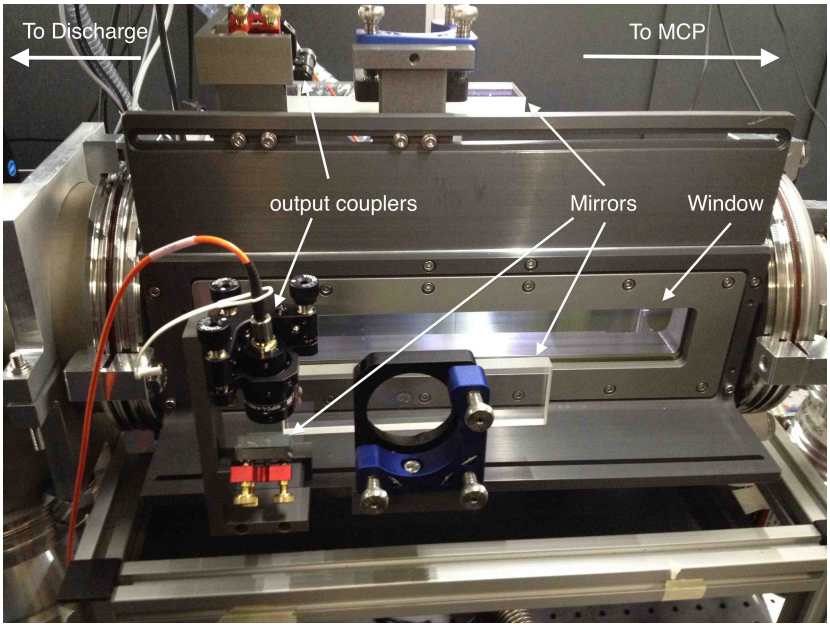

(a)

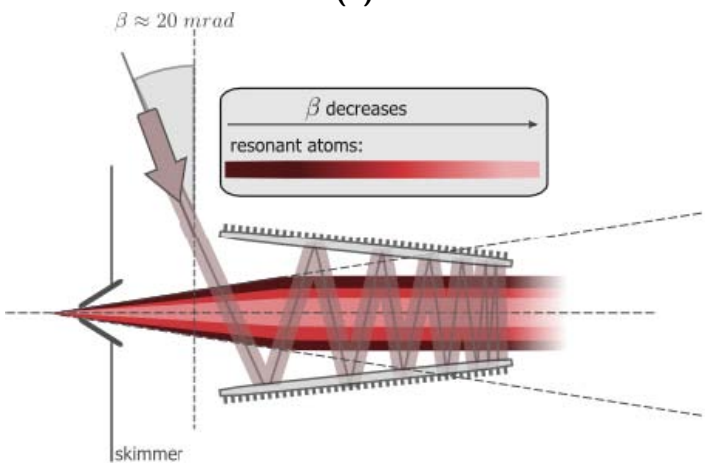

(b)

Figure 5 – (a) picture of the current collimation setup; (b) schematic of the mirror alignment for collimation. Note that the incident angle of the laser beam and the extent of tilting is greatly exaggerated in this picture [14].

3.4 Imaging Setup

To visualize the helium beam, a micro-channel-plate detector (MCP) is placed behind the collimation chamber, about 72 cm from the helium source. The MCP is connected to a pulsed voltage, so that it only captures the metastable helium atoms and does not show photons, ions and electrons that are created in the discharge, before the image on the phosphor screen is captured by a CCD-camera. By connecting the camera to a computer and sending the image to a monitor, we can see a live image of the metastable beam as it appears on the MCP detector. This allows us to adjust the mirrors in real time, which makes aligning the mirrors more efficient [12].

4 Results

4.1 General Predictions

The width of the uncollimated beam of metastable helium atoms can be easily calculated with the distances between skimmers and the MCP. The maximum transverse velocity of helium atoms that are still able to pass the skimmers and reach the MCP is about $32\,\mathrm{ms}^{-1}$, which means that the beam has an uncollimated divergence angle of approximately 2.15° and a diameter of about 28 mm when it reaches the MCP. This prediction is consistent with the observed MCP image, on which the uncollimated beam has a diameter of about $(27.5 \pm 1.0)\,\mathrm{mm}$.

We define the triplet helium beam flux as the number of atoms per steradian and second [7, 8], which has the property of being independent of the distance the beam has traveled. The number of metastable helium atoms entering the collimation chamber can be estimated by calculating what percentage of atoms remain after passing each skimmer. Because these atoms are a mix of singlet and triplet state helium, we need to know how many triplet atoms are created in the discharge; typical values for this are around 90%-95% [7, 8]. The solid angle that encompasses the beam is approximately equal to the area of the cross section of the beam at the MCP divided by the squared distance between MCP and the imagined point of convergence of the divergent helium beam (r). The solid angle can be expressed through the highest transverse velocity inside the helium beam (v_T), its longitudinal velocity (v_L), and the observed beam diameter at the MCP (d) as such:

$$s.a. = \frac{A}{r^2} \approx \frac{\pi(\frac{d}{2})^2}{(\frac{d}{2}\frac{v_L}{v_T})^2} = \frac{\pi v_T^2}{v_L^2} \tag{1}$$

From the source design and our knowledge of the number of atoms being emitted into the source from the helium valve [14], we are able to calculate approximately how many atoms are able to pass the skimmers and reach the MCP (Figure 6). Because the pulse frequency of the helium outlet is 25 Hz, the flux of the uncollimated beam should be around $(1.184 \pm 0.032) \times 10^9\,\mathrm{sr}^{-1}\,\mathrm{s}^{-1}$. We can calculate the theoretical minimum value of the diameter of the collimated beam by assuming that the helium atoms' transverse velocity is reduced to the Doppler-limit when they are being collimated. The Doppler-limit for the $2^3\mathrm{S}_1$ - $2^3\mathrm{P}_2$ transition is given by v_{min}=0.283 ms^{-1}, or equivalently a temperature of $T_{Doppler}$=39 µK. If we assume that the metastable atoms diverge at an angle of 2.15° after they have passed the skimmers, experience a constant laser force along the length of the mirror and then

propagate at a divergence angle determined by the Doppler limit, we calculate an optimal beam diameter after collimation of about $(4.60 \pm 0.19)\,\mathrm{mm}$. Therefore, we expect the ideal collimated beam flux to be $(1.50 \pm 0.04) \times 10^{13}\,\mathrm{sr}^{-1}\ \mathrm{s}^{-1}$. We observed an average collimated beam diameter of $(5.5 \pm 0.5)\,\mathrm{mm}$, which translates to a beam divergence of $(0.10 \pm 0.05)^\circ$ and a transverse velocity of $(1.60 \pm 0.75)\,\mathrm{ms}^{-1}$ (or a temperature on the order of 1 mK). These values were determined by comparing the beam width immediately after collimation (which we can calculate by assuming a constant laser force along the mirror) and the beam width at the MCP. The difference between these two values tells us how large the maximum transverse velocity of the beam is. Using equation (1), we calculated the observed collimated beam flux to be $(5.0 \pm 3.3) \times 10^{11}\,\mathrm{sr}^{-1}\ \mathrm{s}^{-1}$, a 420 ± 282-fold increase compared to the uncollimated beam flux. The large error in the observed beam flux is due to the relatively large error in the transverse velocity of the beam after collimation. The diameter of the collimated beam was determined from the MCP-image and the functions fitted to the MCP data (see Section 4.2).

The observed collimated beam flux is evidently much smaller than the theoretical optimum. This is most likely due to the fact that the helium atoms' transverse velocity is not reduced to the optimal Doppler limit, in addition to detuning and mirror alignment errors. Because the adjustment of the laser detuning and the mirror alignment is done qualitatively by looking at the MCP-image, we can't be sure that our alignment is optimal.

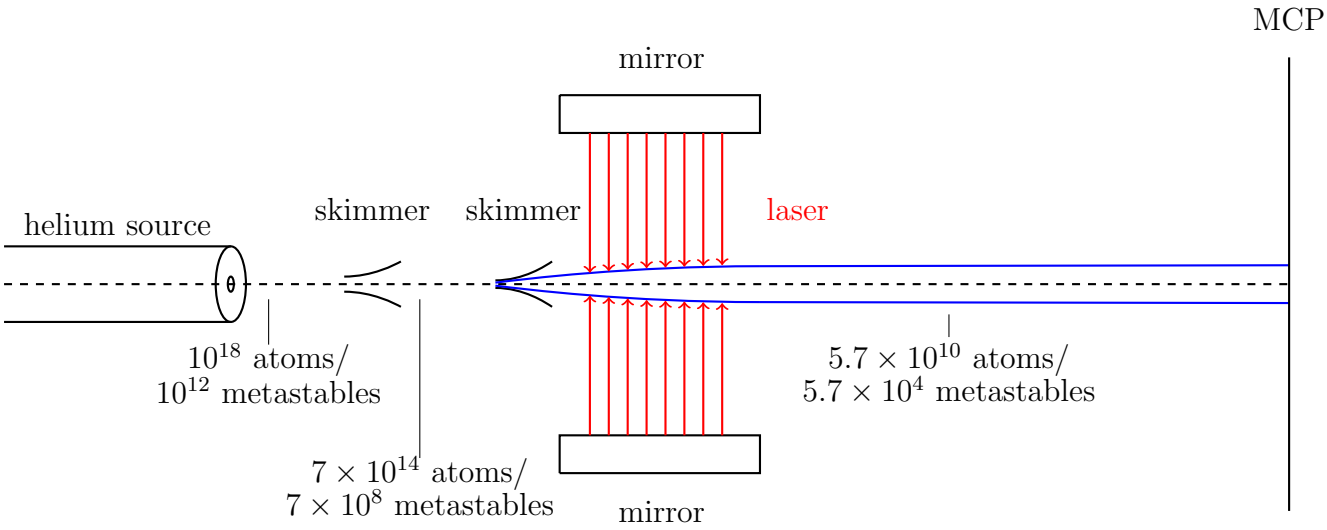

Figure 6 – Expected number of atoms in each section of the source.

4.2 Parameter Variation

To achieve maximal metastable helium beam intensity, we varied some parameters and studied what effect this had on the collimation efficiency. The parameters varied were the laser power, its detuning from atomic resonance and the helium source discharge current, voltage and valve pressure. To quantitatively analyze these changes, the MCP-data was evaluated. The data from the camera was in the form of a matrix, in which each element represented the intensity (in arbitrary units) measured in one pixel. For each measurement a background image (without collimation) and a collimation image (collimated beam) were taken and compared. By subtracting the background data from the data of the collimated beam, we determined to what extent the cooling lasers changed the helium beam intensity and where this intensity change was localized. Figure 7 shows cross sections of the data obtained from the camera in x-direction. Notice that the intensity difference of collimated to background data is negative in a ring around the maximum and positive in the vicinity of the maximum. This indicates that triplet-state helium atoms are being pushed from the edges of the beam towards its center from all sides through the force of the laser. We fitted a one-dimensional gaussian curve to a vertical and horizontal cross section of the background data and multiplied these functions, to obtain a two-dimensional. To fit a function to the background-subtracted collimated beam, we fitted a two-dimensional Lorentzian curve to the positive sections and a two-dimensional Gaussian curve to the negative sections of the camera data and added these. A cross section of the resulting fit and the camera data can be found in Figure 7. This fit allowed us to determine the maximum of the collimated beam and it's FWHM (Full Width at Half Maximum) and their respective errors at the MCP. From these parameters we determined the efficiency of collimation and the optimal source and laser parameters. Because the MCP only shows the metastable helium atoms (see Imaging Setup, Section 3.4), the ratio of the maxima of the background signal (2^3S_1 and 2^1S_0) and the collimated signal (only 2^3S_1) indicates at what ratio singlet-state and triplet-state helium atoms are created in the electric discharge. The FWHM on the other hand is a measure for the beam diameter at the position of the MCP. The errors for the FWHM values were determined by combining the FWHM errors of the Gaussian and Lorentzian functions. This procedure was also used to determine the error of the maxima-ratio.

We also tried to use the fits to the data to determine the efficiency of collimation, i.e. by what percentage intensity increased in the center of the beam and by what percentage intensity decreased around the center. We did this by integrating over the respective areas (i.e. those with negative or positive intensity change) and comparing this with the integral

of the background fit. This procedure however was unsuccessful, since it produced illogical results such as the reduction exceeding the background integral. This might be due to saturation effects, i.e. the MCP is not able to distinguish between two different intensities above a certain threshold. We thus discarded this information and focused on the FWHM and maxima data described above.

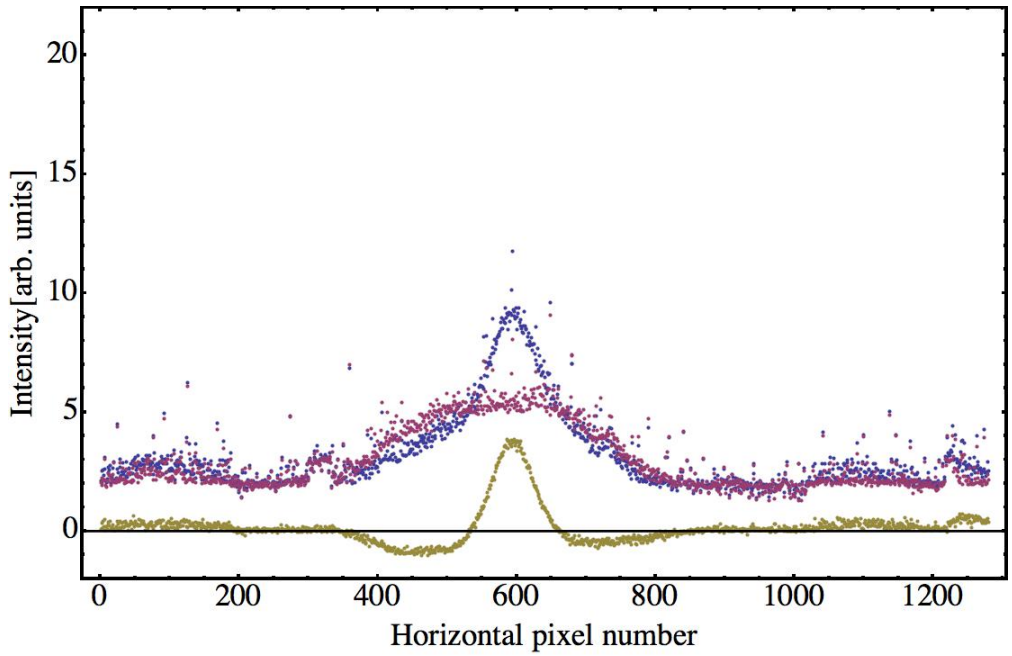

(a)

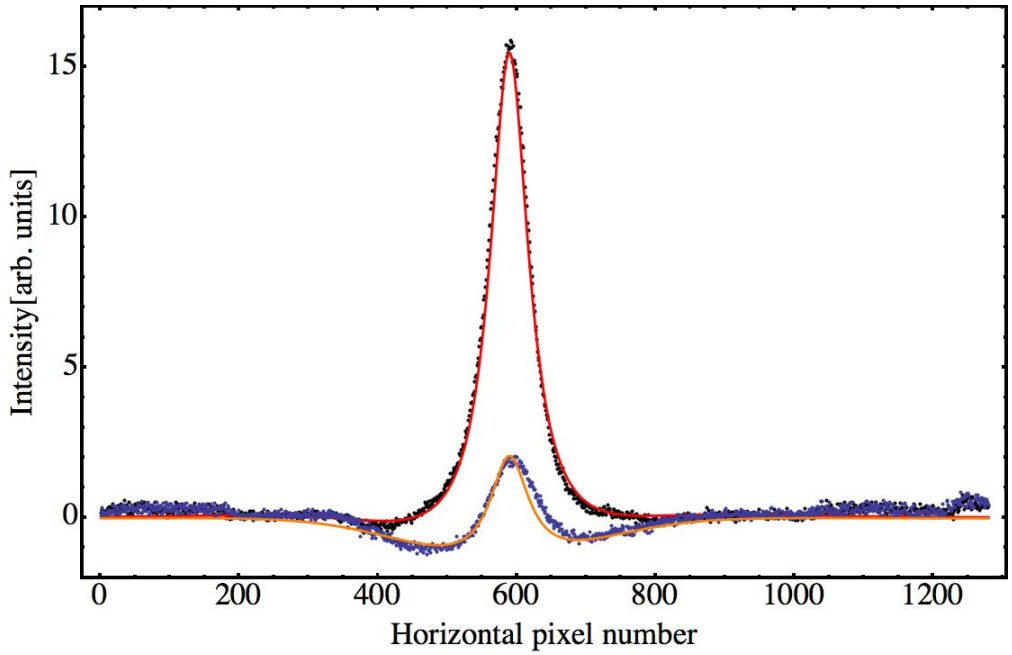

(b)

Figure 7 – (a) Vertical cross section at the 540th horizontal pixel.The background data is red, the collimated beam data blue and the background-subtracted collimation data is yellow. (b) Horizontal cross section of background-subtracted collimation data (black and blue dots) with Gauss-Lorentz Fit (red and orange line). The red fit is approximately given by f(x)=-0.03-1.5exp$[\frac{(x-575)^2}{2(132)^2}]+\frac{20016}{1181+(x-589)^2}$

4.2.1 Detuning

The detuning of the laser can be adjusted by locking onto a slightly off-resonance wavelength when preparing the laser. The detuned laser will be resonant with different transverse velocity classes of the helium atoms (as discussed in Section 2.3), thereby distorting the shape of the helium beam differently than if the laser is resonant in the laboratory frame. A succession of detuning from blue over resonance to red can be seen in Figure 8. If the laser is blue detuned, it will be initially (at first contact) resonant with a smaller transverse velocity group than if the laser were on resonance. Because the laser is blue detuned, the extra blue detuning resulting from the Doppler effect needs to be smaller to achieve resonance, i.e. the resonant velocity group is smaller with larger blue detuning of the laser. This means that the laser can actually "overshoot" towards the end of collimation, becoming resonant with atoms that are slightly divergent, which thus will be receiving a force that increases divergence. The effect can be seen in Figure 8 (a), which shows that the atoms are pushed away from the center of the beam, creating a beam profile whose width is larger than that of the uncollimated beam. If the laser is red detuned, the laser is resonant with higher transverse velocity classes than when the laser is on resonance, due to the Doppler shift needing to be larger (i.e. more blue-detuned) to compensate the red detuned laser. This means that the laser will never be able to affect a transverse velocity group which is smaller than a certain threshold, i.e. collimation is not ideal in that it can not reach the Doppler limit. The beam also takes the rectangular shape of the symmetry of the laser beam, see e.g. Figure 8 (e) & (f) This behavior can clearly be observed on the MCP-images shown in Figure 8. Notice that the collimated beam of the red detuned laser (Figures 8 (e)-(g)) has a round shape, with highest intensity outside the center of the beam. We see that the atoms are pushed from the fringes of the beam to a certain minimum velocity, which is not close to the Doppler limit, creating a ring around the center of the beam.

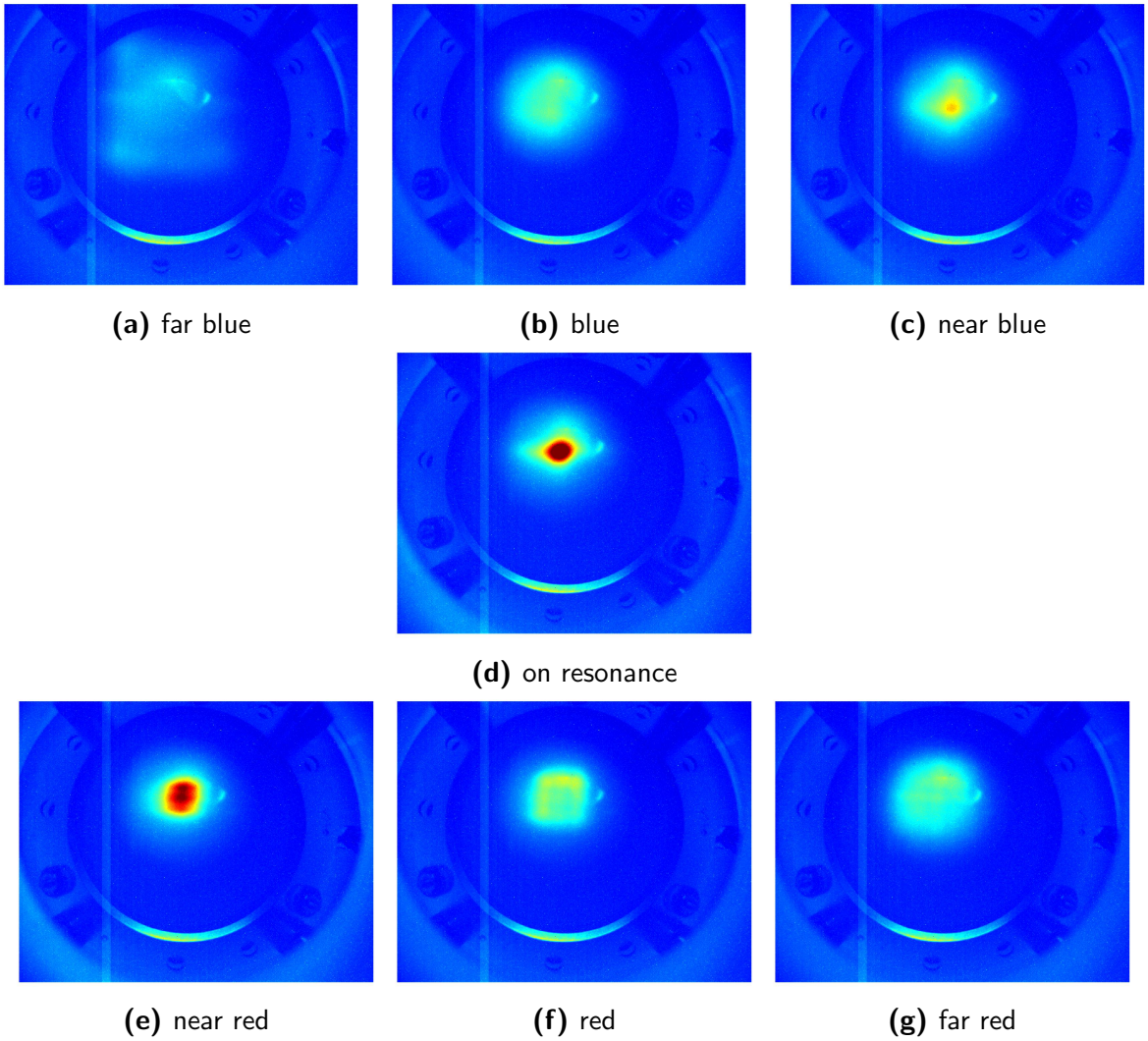

(a) far blue **(b)** blue **(c)** near blue

(d) on resonance

(e) near red **(f)** red **(g)** far red

Figure 8 – Detuning from far blue to far red. Red areas indicate high intensity, blue areas indicate low intensity. The thin ring of high intensity outside the center is caused by stray light reflecting off the metal casing of the MCP. The small spot of intensity, which can be seen on all pictures to the right of the center of the beam is most likely due to a reflection of the laser beam into the camera

4.2.2 Laser Power Variation

The laser's power was changed in a range from 1000 mW to 3000 mW in nonlinear increments by adjusting the diode current in the laser amplifier. By increasing the laser power, we increase the force acting on the helium atoms resulting from laser interaction and increase the linewidth of the optical transition. These effects counteract each other, i.e. higher laser power increases force (reducing beam width) but also increases the line width of the transition, which increases the beam width. Therefore, there should be an optimal power

at which the beam diameter is minimal. The plots (FWHM and maxima-ratio) for laser power variation are shown in Figure 9 (a) and (b). In Figure 9 (a), the outlined prediction of counteracting power effects can be observed. The red line shows a fit that includes power broadening and laser force terms:

$$\mathrm{FWHM}(P) = a\sqrt{1+\frac{P}{b}} - c\frac{P-P_0}{P-d} \tag{2}$$

the first term being due to power broadening [14] and the second due to the dependence of the optical force on laser power [11,12]. The fit in Figure 9 (a) is given by equation (2) with a=2.276, b=891.8, P_0=372, c=0.013 and d=263. Because variation of the laser's power does not influence the singlet/triplet ratio of metastable helium atoms coming from the source, the decrease in maximum ratio in the region 360 mW-650 mW must be due to the broadening of the helium beam (Figure 9 (b)). The data confirms this behavior: An increase in beam width seems to be coupled with a decrease in the collimated beam's maximum. The fit in Figure 9 (b) is given by

$$r(P) = y - mP \tag{3}$$

with m=0.0008 and y=4.92. We conclude that optimal collimation is achieved at a laser power between 350 mW and 400 mW per side after coupling.

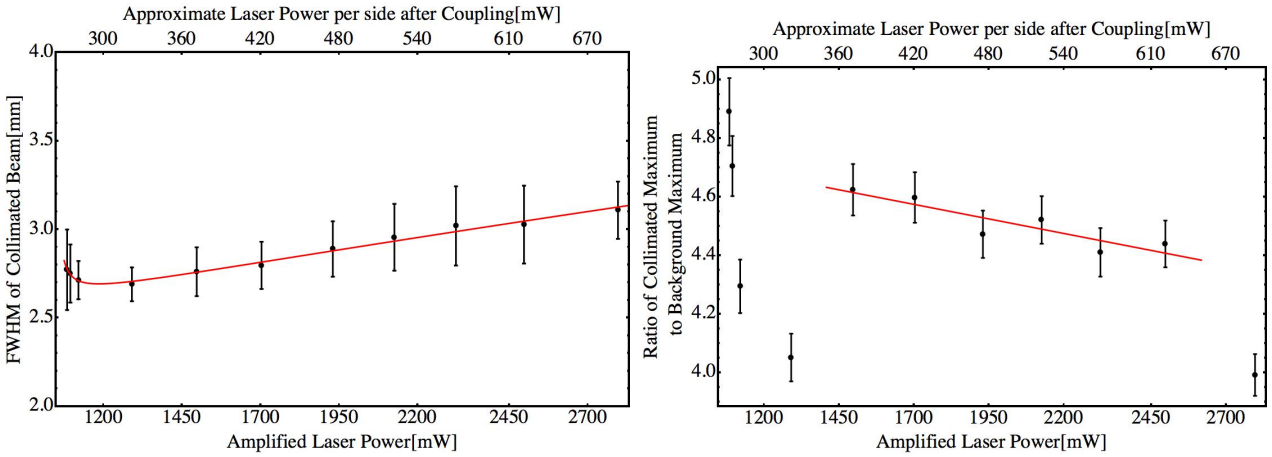

Figure 9 – (a) Dependence of the FWHM of the collimated beam as a function of laser power. The red line is a fit, see equation (2). (b) Dependence of the ratio of collimated maximum to uncollimated maximum as a function of laser power. The red line is a fit, see equation (3).

4.2.3 Discharge Current Variation

The electric discharge current was varied from 0 A to about 6.5 A. However, the discharge only started producing metastable helium atoms when the current was above ≈5 A. Another limiting factor was that the tungsten wire carrying the current broke if the current was too high for too long. This meant that we confined the current measurements to a range of 5 A-6.25 A in steps of 0.25 A. The data for the FWHM and the ratio of the maxima are shown in Figure 10 (a) and (b) respectively. By increasing the electric discharge current, we effectively increase the number of electrons impinging onto the beam of helium atoms. This means that a larger fraction of helium atoms is initially excited to metastable states. Since only the number of metastable helium atoms is changed by current variation and not their longitudinal velocity (which is only determined by geometric constraints), the FWHM of the collimated beam should not be affected. This is also reflected in our data (Figure 10 (a)). The red line shows a fit to the FWHM data:

$$\mathrm{FWHM}(I) = y - mI \tag{4}$$

with m=0.0646 and y=3.6. The current variation has a significant effect on the ratio of the maxima of the collimated and uncollimated beam (Figure 10 (b)), which roughly follows a Lorentzian curve:

$$r(I) = c - \frac{A}{(I - I_0)^2 + \delta I^2} \tag{5}$$

with A=0.352, c=6.05, I_0=5.473 and δI=0.345. From the plots we deduce that the ratio of triplet-state helium to singlet-state helium is lowest at about 5.5 A and increases when lowering or increasing the discharge current. A higher discharge current therefore seems to be advantageous for creating a high triplet-state helium beam flux. The data seems to reveal an increased production of metastable singlet helium atoms at a current of ≈5.5 A.

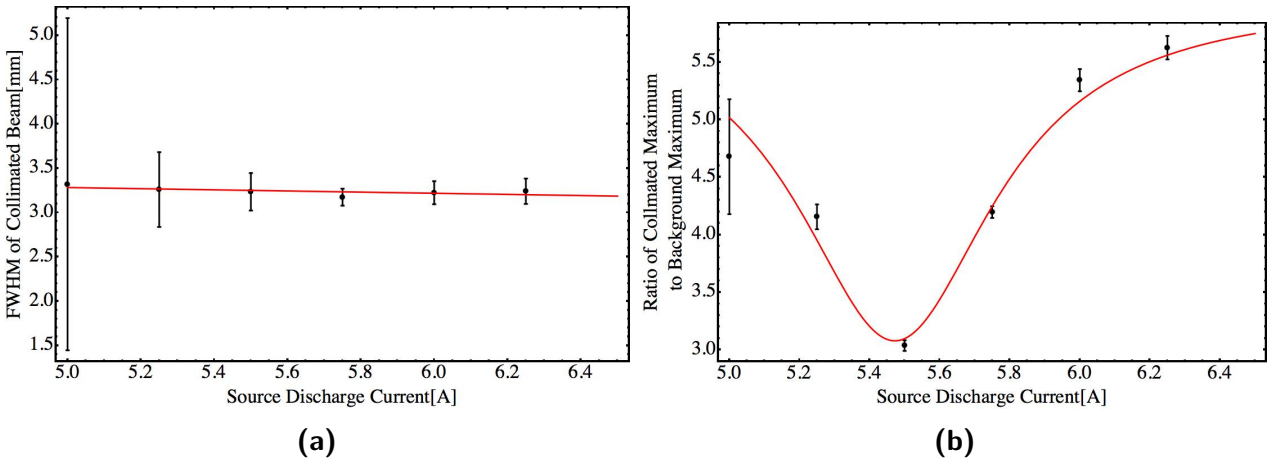

Figure 10 – (a) Dependence of the FWHM of the collimated beam as a function of AC source current. the red line is a fit, see equation (4). (b) Dependence of the ratio of collimated maximum to uncollimated maximum as a function of AC source current. The red line is a fit, see equation (5).

4.2.4 Discharge Voltage Variation

The voltage of the anode of the electric discharge was varied from 200 V to 350 V in steps of 30 V. By increasing the discharge voltage we effectively increase the kinetic energy of the electrons impinging onto the beam of helium atoms. As with the current variation, the FWHM remains largely unaffected by voltage variations (Figure 11 (a)). The red line is a fit to the FWHM-data given by

$$\mathrm{FWHM}(V) = y + mV \tag{6}$$

with y=3.164 and m=0.0067. This is also due to the fact that voltage variation does not change the characteristics of collimation, but only of the singlet-triplet-ratio. The ratio of maxima (Figure 11 (b)) is also relatively constant with voltage variation. The deviations at 200 V and 350 V are due to instabilities in the discharge process. The electric discharge voltage therefore has no significant effect on the production of metastable helium atoms or on collimation.

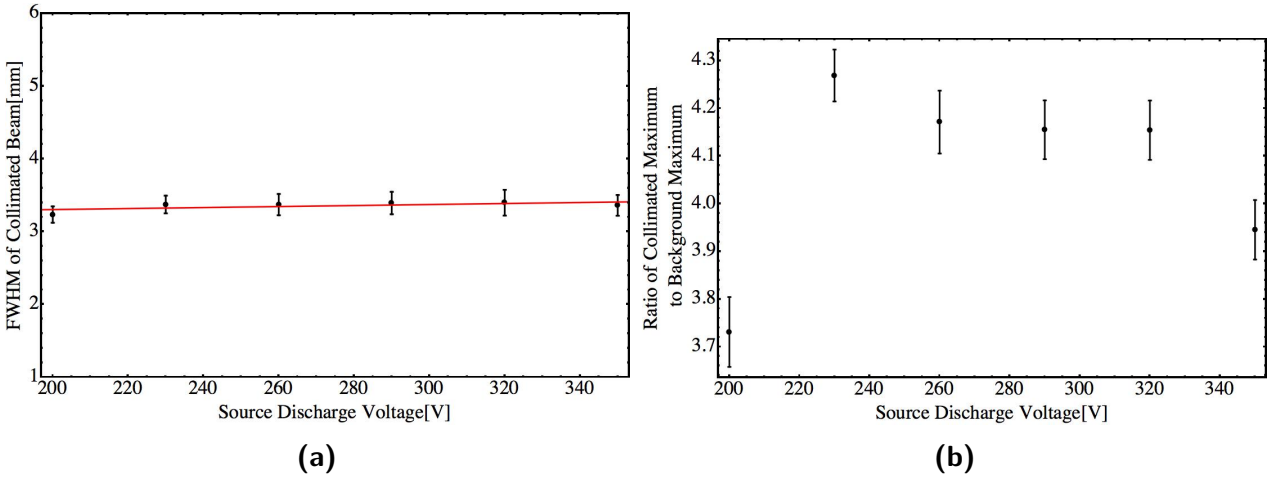

Figure 11 – (a) Dependence of the FWHM of the collimated beam as a function of discharge voltage.The red line shows a fit, see equation (6). (b) Dependence of the ratio of collimated maximum to uncollimated maximum as a function of discharge voltage.

4.2.5 Helium Pressure Variation

We varied the pressure of the stream of helium atoms into the discharge chamber from 1.5×10^{-5} mbar to 6×10^{-5} mbar in increments of 0.5×10^{-5} mbar. This was done by slightly opening the valve connecting the helium canister and the metal tube leading into the discharge chamber. This procedure changes the density/number of helium atoms that enter the discharge chamber and the extent of collisions with background gases. The higher the valve pressure, the larger the density in the beam of helium atoms. As with the variation of discharge current and voltage, we observed no effect on the FWHM when changing the valve pressure (see Figure 12 (a)). Our fit for this dependence is given by

$$\mathrm{FWHM}(p) = y - mp \tag{7}$$

with m=0.0095 and y=3.4, which indicates a negligible linear decrease in FWHM of 0.0095 millimeters per 10^{-5} millibar. The ratio of maximas however seems to follow a square root function (see Figure 12 (b)), indicating that a higher valve pressure leads to a small increase in triplet-state helium production. The red line shows a fit to:

$$r(p) = c + a\sqrt{p - p_0} \tag{8}$$

with c=3.86, a=0.61 and p_0=1.5.

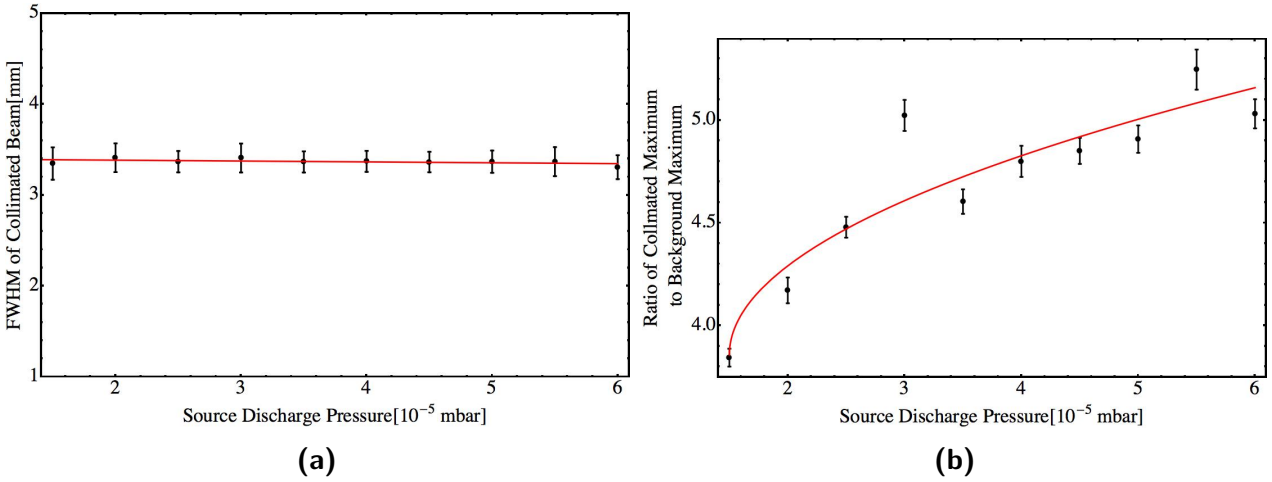

(a) **(b)**

Figure 12 – (a) Dependence of the FWHM of the collimated beam as a function of chamber pressure. The red line is a fit for the FWHM, see equation (7). (b) Dependence of the ratio of collimated maximum to uncollimated maximum as a function of chamber pressure. The red line shows a fit for this ratio, see equation (8).

5 Conclusion

We demonstrated that we can effectively collimate metastable triplet-state helium atoms. The observed collimated beam flux is probably close to the maximum achievable, but might be increased by choosing the optimal parameters for the laser and electric discharge. From our parameter variation experiments (section 4.2), we deduce that we can maximize our triplet-state helium beam flux with a discharge current between 5.75 A and 6 A, a discharge voltage between 200 V and 300 V, a discharge pressure of about 4.5×10^{-5} mbar and a laser power of 350 mW and 400 mW per side after coupling. The diode current in the amplifier should therefore have a value between 500 mA and 700 mA.

5.1 Outlook

Another Semester student is currently working on deflecting the triplet-state helium atoms [6], so as to create a pure, uncontaminated beam of metastable triplet helium. Once this has been accomplished, we will need to connect the entire helium source (including the collimation and deflection setup) to the main experiment. This could be challenging because we are not able to rely on an MCP-image to adjust the incidence of the beam into the experiment chamber. To account for the new type of atoms (triplet-state instead of singlet-state), we will need to exchange the laser setup in the main experiment, so that the lasers are resonant with the triplet-state helium transitions.

6 Appendices

6.1 Appendix A: Doppler Detuning

We can imagine an atom moving freely through space with a velocity $\vec{v}$ and a photon impinging onto this atom, with a frequency f and a wave vector $\vec{k}$. Through the Doppler shift, the atom will observe the wavelength of the photon to be

$$\lambda = \lambda_0 + \frac{\vec{v}\vec{k}}{|\vec{v}||\vec{k}|}|\vec{v}|T_0 = \lambda_0 + \frac{\vec{v}\vec{k}}{|\vec{k}|}T_0,$$

where λ_0 and T_0 are the wavelength and oscillation period of the photon observed in the laboratory frame respectively. The frequency of an electromagnetic wave in vacuum is given by the speed of light c divided by the wavelength of the wave. This means that the atom observes the photon to have a frequency of

$$f = \frac{c}{\lambda_0 + \frac{\vec{v}\vec{k}}{|\vec{k}|}T_0} = \frac{1}{\frac{\lambda_0}{c} + \frac{\vec{v}\vec{k}}{c|\vec{k}|}T_0} = \frac{1}{\frac{1}{f_0} + \frac{\vec{v}\vec{k}}{c|\vec{k}|}\frac{1}{f_0}} = \frac{f_0}{1 + \frac{\vec{v}\vec{k}}{c|\vec{k}|}} \tag{9}$$

For $|\vec{v}| \ll c$ we can approximate f with the first-order Taylor expansion of (9):

$$f \approx f_0(1 - \frac{\vec{v}\vec{k}}{c|\vec{k}|}) = f_0 - \frac{\vec{v}\vec{k}}{\lambda|\vec{k}|} = f_0 - \frac{\vec{v}\vec{k}}{2\pi}$$

$$\rightarrow \omega = 2\pi f = \omega_0 - \vec{v}\vec{k}$$

$$\rightarrow \delta = -\vec{v}\vec{k}$$

References

[1] S. D. Hogan, J. A. Agner, T. Thiele, and S. Filipp. Driving rydberg-rydberg transitions from a co-planar microwave waveguide. *Physical Review Letters*, 2012.

[2] T. Thiele, S. Filipp, and J. A. Agner. Manipulating rydberg atoms close to surfaces at cryogenic temperatures. *Physical Review A*, 2014.

[3] C. J. Foot. *Atomic Physics*. Oxford University Press, 2005.

[4] S. S. Hodgman, R. G. Dall, L. J. Byron, K. G. H. Baldwin, S. J. Buckman, and A. G. Truscott. Metastable helium: A new determination of the longest atomic excited-state lifetime. *Physical Review Letters*, 103(053002), 2009.

[5] R. S. Van Dyck, Jr., C. E. Johnson, and H. A. Shugart. Radiative lifetime of the 2 $^1S_0$ metastable state of helium. *Physical Review A: Atomic, Molecular and Optical Physics*, 4(1327), 1971.

[6] D. Friese. Deflection of metastable helium via laser light. Semester Thesis, 2014. ETH Zurich/Quantum Device Lab.

[7] T. Halfmann, J. Koensgen, and K. Bergmann. A source for a high-intensity pulsed beam of metastable helium atoms. *Measurement Science and Technology*, 2000.

[8] G. R. Woestenenk. Construction of a low velocity metastable helium atomic beam. *Review of Scientific Instruments*, 72(10), 2001.

[9] T. F. Gallagher. *Rydberg Atoms*. Cambridge University Press, 2005.

[10] L. Marmet. NRC's cesium fountain clock. `http://archive.nrc-cnrc.gc.ca/eng/projects/inms/fountain-clock.html`, 2010. [Online; accessed 16-June-2014].

[11] T. Thiele. Towards a manipulation of trapped atoms in optical tweezers. Master's thesis, ETH Zürich, 2013.

[12] L. Gerster. Metastable helium source. Semester Thesis, 2014. ETH Zurich/Quantum Device Lab.

[13] E. D. Black. An introduction to pound-drever-hall laser frequency stabilization. *American Journal of Physics*, 69(1), 2001.

[14] A. Hambitzer. Notes on the project "helium source 2013". Unfinished report outlining the details of the triplet-state helium source, 2013.

Eidgenössische Technische Hochschule Zürich
Swiss Federal Institute of Technology Zurich

Declaration of originality

The signed declaration of originality is a component of every semester paper, Bachelor's thesis, Master's thesis and any other degree paper undertaken during the course of studies, including the respective electronic versions.

Lecturers may also require a declaration of originality for other written papers compiled for their courses.

I hereby confirm that I am the sole author of the written work here enclosed and that I have compiled it in my own words. Parts excepted are corrections of form and content by the supervisor.

Title of work (in block letters):

Collimation of metastable 2 ^3S_1 helium atoms using laser cooling techniques

Authored by (in block letters):
For papers written by groups the names of all authors are required.

Name(s):	**First name(s):**
Melchner von Dydiowa	Max

With my signature I confirm that

- I have committed none of the forms of plagiarism described in the 'Citation etiquette' information sheet.
- I have documented all methods, data and processes truthfully.
- I have not manipulated any data.
- I have mentioned all persons who were significant facilitators of the work.

I am aware that the work may be screened electronically for plagiarism.

Place, date	**Signature(s)**
ETH Zurich, 03.07.14	M Melchner

For papers written by groups the names of all authors are required. Their signatures collectively guarantee the entire content of the written paper.